

Photopolymerizable Hybrid Sol-gel: New Opportunities for UV-cured Coatings

Céline Croutxé-Barghorn^{1*}, Abraham Chemtob¹, Davy-Louis Versace¹, Cindy Belon¹, Séverinne Rigole²

¹*Department of Photochemistry, CNRS UMR 7525
University of Haute-Alsace, ENSCMu,
3, rue Alfred Werner 68093 Mulhouse Cedex, France*

²*Laboratoire des Matériaux à Porosité Contrôlée, CNRS UMR 7016
University of Haute-Alsace, ENSCMu,
3, rue Alfred Werner 68093 Mulhouse Cedex, France*

Abstract

Photopolymerizable organic-inorganic sol-gel coatings combine numerous advantages: good adhesion to substrates, abrasion and chemical resistance. Owing to the possibility of controlling the inorganic network density, sol-gel films can also form an effective barrier layer. Crackability is limited by the presence of the organic component. The present paper focuses on the new opportunities opened by these materials in the UV-curing field in terms of photopolymerization process and final coatings properties.

I. Introduction

Polymer nanocomposite science is a very dynamic and emerging field in polymer chemistry. Like other polymerization processes, photopolymerization has known a recent explosion of research in this area. UV-cured organic-inorganic hybrid materials generally attempt at combining hardness, flexibility and resistance to chemicals, scratch, heat, while maintaining transparency and gloss. Major applications in this field are abrasion resistant coatings^{1,2}, protective films for plastics providing barrier properties^{3,4}, glass coatings⁵ and novel optical devices⁶. Two synthetic pathways have been mainly developed for the preparation of UV-curable nanocomposites.

The first method mainly relies on low molecular weight organoalkoxysilanes $R'Si(OR)_3$ as one or more of the precursors for the sol-gel reaction, with R' a photopolymerizable organic function via radical or cationic means^{7,8,9,10,11,12}. A preliminary sol-gel step produces a liquid organic-based polysiloxane network that can be photopolymerized subsequently, affording a solid cross-linked organic-inorganic system.

The second strategy uses preformed inorganic nanoparticles which are dispersed into photocurable monomers^{13,14}. A great deal of examples lies on photoinduced free radical polymerization of multifunctional acrylates incorporating either colloidal or fumed silica^{15,16,17,18}. In addition to SiO_2 , the influence of other equi-axed nanoparticule fillers¹⁹ (TiO_2 , AlO_3 , etc) and plate-like nanofillers (smectic clays or phyllosilicates) have been evaluated within various UV curing formulations²⁰.

* Celine.Croutxe-Barghorn@uha.fr; tel: + 33 389 335 017; fax: + 33 389 335 014

In this work, a novel one-step methodology for preparing hybrid sol-gel coating has been investigated by UV irradiation of simple and commercial bifunctional hybrid precursors, bearing both an organic epoxy function and alkoxy silane moieties, in presence of an aryl iodonium salt. Through the in situ liberation of protic acids via onium salt photolysis, polymerization of epoxides takes place concomitantly with hydrolysis and condensation of the reactive silanes. This straightforward method gives access to a stable, solvent-free and single-component hybrid coating composition, which can be applied at room temperature and cured upon UV exposure.

The present paper first focuses on a study of the organic and inorganic photopolymerization by Fourier Transform Real-Time Infrared spectroscopy (FT-RTIR). Then, the hybrid network microstructure was characterized by ^{29}Si and ^{13}C NMR spectroscopy. A particular effort was made to understand how the hybrid structure is affected by the two concurrent polymerization processes.

II. Experimental

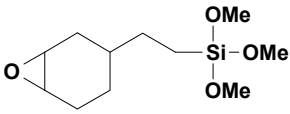
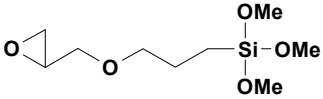
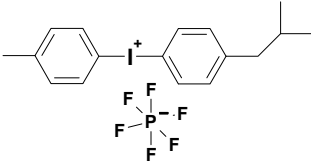
II.1 Materials and Preparation of hybrid sol-gel films

3-(glycidyloxypropyl)trimethoxysilane (GPTMS) and [2-(3,4-epoxycyclohexyl)ethyl] trimethoxysilane (TRIMO) were used without further purification. (4-methylphenyl)[4-(2-methylpropyl) phenyl] iodonium hexafluorophosphate, which behaves both as a photoinitiator for the organic and inorganic moieties is a 75% solution of the active substance in propylene carbonate. The structure of GPTMS and TRIMO-based silanes were given in Table 1.

For the dual inorganic-organic UV-curing, GPTMS or TRIMO were readily mixed with 2% wt. of photoinitiator. The homogeneous solution was then coated onto BaF_2 pellet prior to irradiation under UV-light.

In a conventional sol-gel procedure, the organosilane precursor was hydrolyzed with an acidified water solution. A water to silicon ratio (r_w) of 3 as well as an acid concentration of 0.1 Mol/L were chosen. The mixture was allowed to mature for 72h. Partial elaboration of the silicate backbone was thus achieved.

Table 1. Structure of the bifunctional hybrid monomers and the cationic photoinitiator

COMPOUND	FUNCTION	STRUCTURE
2-(3,4-epoxy-cyclohexylethyl)trimethoxysilane TRIMO	Hybrid monomer	
(3-glycidyloxypropyl) trimethoxysilane GPTMS	Hybrid monomer	
(4-methylphenyl)[4-(2-methylpropyl) phenyl] iodonium hexafluorophosphate	Photoinitiator	

II.2 RT FTIR spectroscopy

The photochemical process taking place under illumination was followed by Fourier transform real-time infrared spectroscopy (FT-RTIR). The irradiation source was a Hg-Xe lamp (150W, irradiance of 200 mW/cm²) coupled with a light-guide, transparent to near UV and visible light. Infrared spectra were recorded with a FTIR spectrometer). All photosensitive materials were coated onto BaF₂ chips to display a similar thickness of 3 μm.

II.3 NMR spectroscopy

Liquid and solid state NMR measurements were performed on a Bruker MSL 400-spectrometer. Liquid ²⁹Si NMR experiments (79.48 MHz) were recorded at room temperature with a 6.7 or 10.5 μs pulse width (π/4). The single pulse high power decoupling (HP/DEC) ²⁹Si MAS and ¹³C MAS spectra were collected with a spinning rate of 4000 rpm and delay time of 80 s.

III. Results and discussion

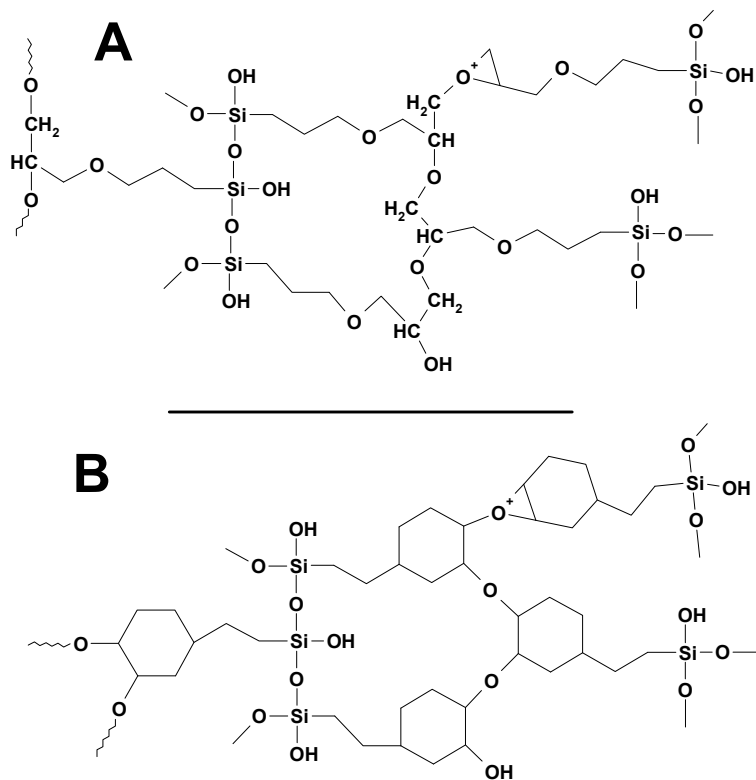
III.1 Dual UV-curing kinetics of epoxy trialkoxysilane hybrid monomers

The alkoxy silane precursors were irradiated in the presence of photoacids generated through UV-decomposition of the photoinitiator, leading in both cases to transparent and homogeneous films with a gel content of nearly 100%. (4-methylphenyl)[4-(2-methylpropyl) phenyl] iodonium hexafluorophosphate is well-known in the literature to be a very efficient cationic photoinitiator for the ring-opening polymerization of epoxy. Scheme 1 outlines an idealized structure of the hybrid interpenetrating networks formed by simultaneous reaction of the inorganic and organic parts of TRIMO and GPTMS.

The photolysis of the photoinitiator generates the very powerful superacid HPF₆, enabling two types of reaction:

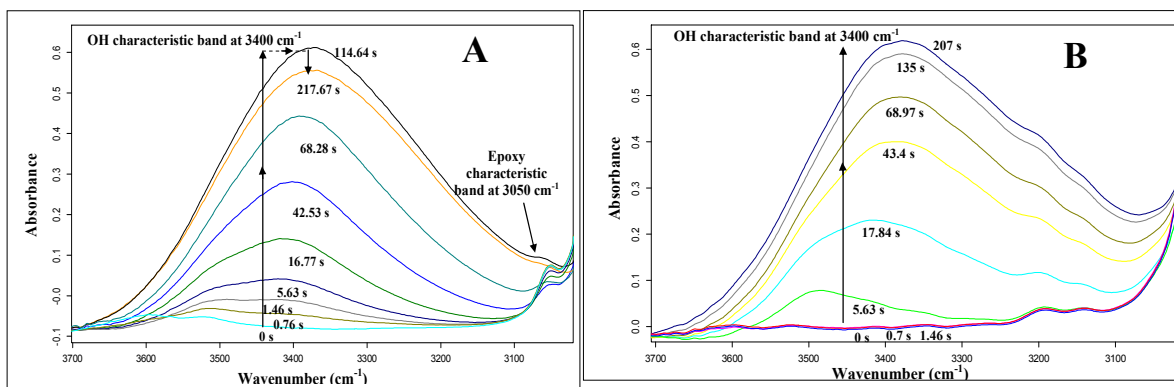
Epoxy protonation takes place through a rapid and quantitative process. A series of chain-propagation then follows via epoxy ring-opening, affording a linear poly(ethylene oxide) (PEO).

Superacids are effective in catalyzing sol-gel reactions. The mechanism of the HPF₆-catalyzed reaction is similar to that of a conventional HCl-catalyzed process. Basically, it proceeds as a two-step network-forming polymerization. Alkoxy functions (SiOR) are first hydrolyzed to generate silanol intermediate species (SiOH). These latter can then undergo a stepwise polycondensation reaction to form a three-dimensional silica network (Si-O-Si). In contrast to typical sol-gel process, there is no water in the present UV-curable system. Traces of water from air moisture appear to be sufficient to initiate the hydrolysis reactions. The sol-gel polymerization of trialkoxysilanes such as TRIMO or GPTMS is known to result in the formation of polysilsequioxane (polySSQO) (RSiO_{3/2})_n products denoted T_n. PolySSQOs consist in a mixture of linear, branched and also cyclic polyhedral structures.



Scheme 1. Type of the organic-organic hybrid network formed by the dual photocrosslinking of GPTMS (A) and TRIMO (B)

RT-FTIR is a very powerful technique to investigate the formation of the hybrid network formation as a function of the irradiation time. Figure 1A shows the RT-FTIR absorption spectrum (between 3700 and 3000 cm^{-1}) of the GPTMS sample throughout the UV irradiation. This spectral region assigned to O-H stretching vibrations substantially evolves under UV irradiation. After only one second of UV treatment, a significant increase in intensity is visible in conjunction with a shift towards lower wavenumbers, which can be attributed to the transition from isolated silanols (3700-3500 cm^{-1}) to hydrogen-bonded silanols (3650-3200 cm^{-1}). Further exposition to UV light gives rise to a broad and intense band around 3400 cm^{-1} , whose presence can be explained by the photoacid-catalyzed hydrolysis of SiOMe groups resulting in the formation of SiOH functions. Other phenomena support this result: the disappearance of the band at 2840 cm^{-1} characteristic of the methoxysilyl groups and a broadening peak around 910 cm^{-1} due to SiOH stretching vibrations. After 114 s of exposition, the broad band centered near 3400 cm^{-1} starts decreasing in intensity. This may be the sign of important condensation reactions of silanol groups followed by elimination of water or methanol molecules. In agreement with this, is the appearance of an intense peak around 1100 cm^{-1} that was assigned to Si-O-Si asymmetric stretching vibrations. In addition, a slow decrease of the band at 3050 cm^{-1} attributed to the epoxy groups can be observed on the FTIR spectrum. Besides showing the low reactivity of the glycidyl ether function of GPTMS, this last result brings the evidence that epoxy ring-opening occurs concomitantly and quantitatively with the photo-induced sol-gel process. As can be seen in Figure 1B, a similar RT-FTIR analysis conducted with TRIMO led to different results. First, the OH band significantly increases upon UV exposure until it levels off without exhibiting a decreasing phase. Last, TRIMO does not give birth to a clear absorption band at 3050 cm^{-1} .

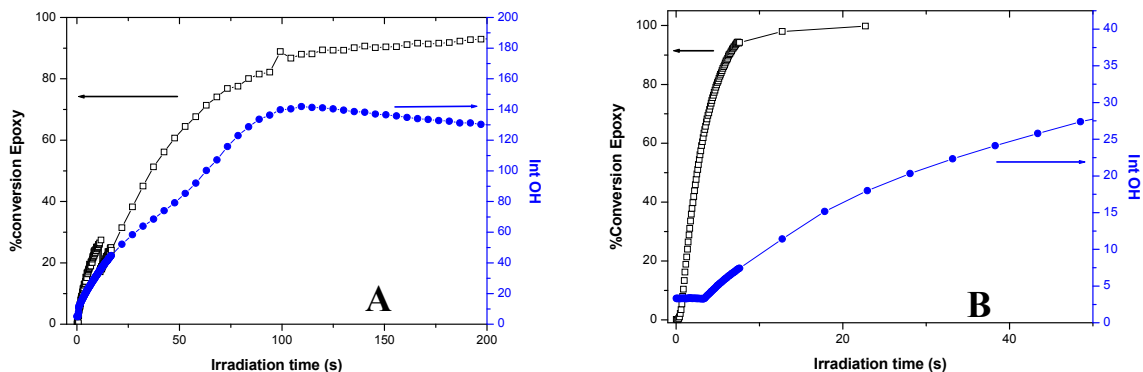


Figures 1A and 1B. RT-FTIR spectra of GPTMS (A) and TRIMO (B) samples between 3700 and 3000 cm^{-1} throughout UV irradiation

Figures 2A and 2B show the conversion of epoxy functions and the extent of hydrolysis reactions (I_{OH}) respectively in the GPTMS and TRIMO samples. Without being quantitative, the ratio between the intensity of the band at 3400 cm^{-1} and a reference peak at 1193 cm^{-1} corresponding to Si-CH₂ stretching can give interesting insight into the sol-gel reactions. Epoxy conversion throughout the UV illumination was determined by monitoring the decrease in area of characteristic absorption bands. For GPTMS, the evolution of the band at 3050 cm^{-1} (C-H epoxy stretch) was followed whereas that located at 910 cm^{-1} (asymmetrical ring stretch) was chosen in the TRIMO samples.

As shown graphically, the type of hybrid monomer has a strong impact not only on the epoxy cationic polymerization but also on the sol-gel kinetics.

- The monomer bearing an epoxylohexyl group displays a much higher reactivity than that containing an epoxyether: conversion in epoxy from TRIMO reaches 90% after 6 seconds of UV polymerization in contrast to 135 seconds in the case of GPTMS. Complete epoxy consumption was also achieved with this highly reactive precursor whereas a limiting conversion around 92% was observed with GPTMS.
- GPTMS gives a valuable example of true concomitant organic inorganic UV-polymerization. In this case, sol-gel process and organic polymerization are efficiently catalyzed by photoacids in a synchronous way. TRIMO exhibits a very different behaviour since hydrolysis becomes active subsequently to the reaction of the greatest part of the epoxy groups. Sign of absorbance at 3400 cm^{-1} indeed appears after 3.5 s when almost 70% of epoxy functional groups have been already converted. This would tend to suggest that the dual UV curing of TRIMO proceeds in a stepwise manner: a poly(ethylene oxide)-based polymer including trialkosyl functions was first synthesized before being subjected to sol-gel reactions.
- Inorganic photopolymerization of GPTMS can be clearly distinguished from that of TRIMO by a marked decrease in intensity of the OH band after 110s of illumination. This has led to assume that a higher degree of condensation in the oxo-silica network might be achieved with this monomer.



Figures 2A and 2B. Epoxy conversion-time curve (Left axis) for the cationic photopolymerization of GPTMS (A) and TRIMO (B). Hydrolysis extent in both monomers as a function of the irradiation time (right axis) monitored by the ratio between the intensity of the band at 3400 cm^{-1} and a reference peak at 1193 cm^{-1} .

III.2 Study of hybrid network microstructure by ^{29}Si and ^{13}C NMR spectroscopy

Solid state NMR spectroscopy has been implemented to investigate the structure of the hybrid material subsequently to the dual UV curing of GPTMS and TRIMO. Quantitative NMR analysis was carried out in all cases through high power decoupling (HP/DEC) experiments. ^{29}Si NMR is well-suited to the investigation of the structure of the oxo-silica. Table 2 summarizes the different environments at a silicon centre (T_i) depending on the degree of condensation. In trialkoxysilane precursors, T_i indicates the fraction of the units with i siloxane bonds $-\text{O}-\text{Si}-$ attached to the central silicon. Given all these sub-structures can be distinguished in a ^{29}Si NMR spectrum, one can have access to the degree of condensation in the siloxane network. ^{13}C NMR is a complementary technique since the different opening reactions of epoxy rings can be distinguished.

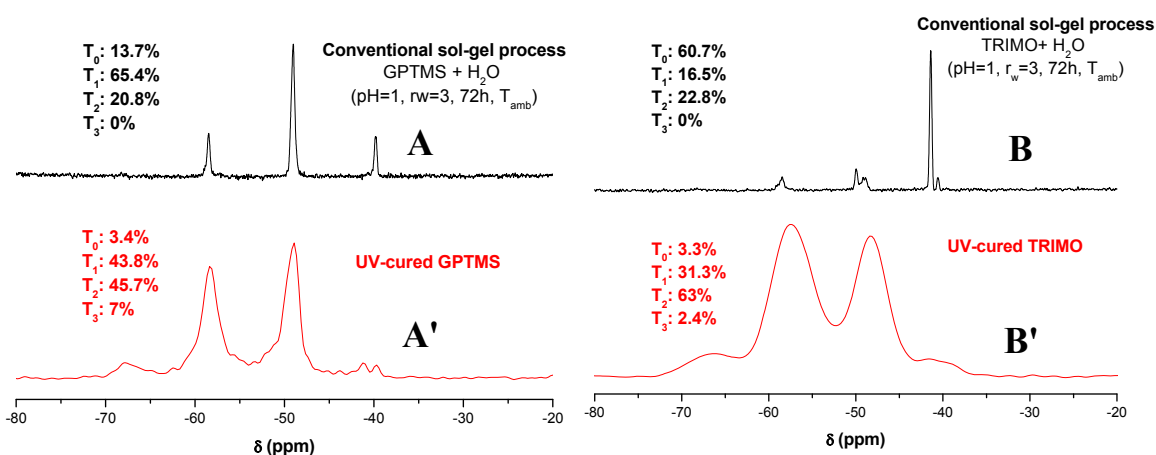
Table 2. Typical ^{29}Si NMR signals of silica atoms appearing in oxo-silica structures originated from trialkoxysilanes.

	T^0 sub-structure	T^1 sub-structure	T^2 sub-structure	T^3 sub-structure
δ_{Si} in ppm	-41 to -43	-48 to -52	-54 to -61	-64 to -69
Structure	$\begin{array}{c} \text{OH} \\ \\ \text{MeO}-\text{Si}-\text{OH} \\ \\ \text{R} \end{array}$	$\begin{array}{c} \text{OH} \\ \\ \text{MeO}-\text{Si}-\text{O}-\text{Si} \\ \quad \\ \text{R} \quad \text{---} \end{array}$	$\begin{array}{c} \text{OH} \\ \\ \text{---Si}-\text{O}-\text{Si}-\text{O}-\text{Si---} \\ \quad \quad \\ \quad \quad \text{R} \quad \quad \quad \end{array}$	$\begin{array}{c} \text{---Si---} \\ \\ \text{O} \\ \\ \text{---Si---O---Si---O---Si---} \\ \quad \quad \\ \quad \quad \text{R} \quad \quad \quad \end{array}$

III.2.1 Effect of the photoacids on the structure of the oxo-silica inorganic network

Figure 3A' shows the solid-state ^{29}Si NMR spectrum of a UV-cured GPTMS sample. The inorganic network was made up mainly of T_1 and T_2 siloxanes sub-structures, with a minor contribution from T_0 and T_3 . Even though the network formed is not highly cross-linked, this clearly proves that UV-generated Brønsted acids are efficient in promoting sol-gel condensation reactions. This result was also compared to that of a sample (Figure 3A) obtained by liquid ^{29}Si NMR in which GPTMS was subjected

to a sol-gel condensation for 72h in a HCl aqueous solution (water to silicon ratio (r_w) = 3, pH=1). Interestingly, the relative amount of T_2 in the UV-cured was found to be more than twice that obtained with a conventional sol-gel process. Upon replacing GPTMS by TRIMO, similar conclusions were reported (Figures 3B and 3B'). As observed previously, UV curing promotes a higher degree of condensation in the inorganic network: di-substituted siloxane linkages are mostly formed through a photoacid-catalyzed sol-gel process versus essentially monomeric species (T_0) in acidic solution. Although, UV polymerized samples resulting from TRIMO and GPTMS displayed comparable degrees of condensation, this structural similarity is not reflected in the evolution of the OH absorption band given by RT-FTIR experiments. Discrepancies between both monomers may be ascribed to the "burying" of volatile water or methanol species resulting from condensation reactions. It is also plausible that alcohol molecules can positively interfere with the photoinitiated cationic polymerization of epoxy, as recently stated in the literature.



Figures 3. Liquid state ^{29}Si CP/MAS NMR experiments were recorded for the conventional sol-gel process of GPTMS (A) and TRIMO (B) (pH=1, r_w =3, t_{reaction} =72h, T_{amb}). Solid state ^{29}Si HP/DEC spectra of UV-cured GPTMS (A') and TRIMO (B') were performed.

III.2.2 Effect of the photoacids on the structure of the polyether organic network

^{13}C high power decoupling (HP/DEC) and ^{13}C CP/MAS NMR experiments were performed respectively with the UV-polymerized organosilanes as well as the unreacted precursors. Compared to the monomers, the UV-cured samples exhibit a broad and intense peak around 75 ppm readily related to the formation of oligo- or poly(ethylene oxide) chains via ring-opening reactions of the epoxy functions. For TRIMO, the absence of signals corresponding to the carbons of the epoxy ring around 50 ppm is in itself the firm evidence that a complete opening of the epoxy has been accomplished. For GPTMS, an epoxy conversion rate of 85% was estimated by ^{13}C NMR, which is in concordance with the result obtained by RT-FTIR (92%).

IV. Conclusion

Onium salts are well-known for use in the chain photopolymerization of epoxy, vinyl ether and other cationically-curable groups. Their utility in catalyzing the sol-gel process of reactive silanes has not been extensively recognized. In this work, we described the dual organic-inorganic UV-curing of ambifunctional hybrid precursors such as GPTMS and TRIMO, including both an organic epoxy

function and a trialkoxysilane group. Dual UV curing implies that hybrid networks are prepared by simultaneous formation of inorganic and organic phases through the catalysis of photoacids formed by photolytic degradation of aryl iodonium salts.

Traditionally, by using organically-modified alkoxy silane, the organic network build-up occurs within a preformed sol-gel inorganic network which imposes restrictions on the molecular movement. Dual UV curing has allowed remarkable epoxy conversion rates combined with a high degree of condensation for the inorganic part. Other authors have studied the concept of ambifunctional monomer but they all resorted to conventional acid or basic catalysts. Compounds such as (γ -aminopropyl)triethoxysilane, BF_3 and various metal transition alkoxides enabled both siloxane formation and epoxy ring-opening polymerization. However, their lack of latency prevents their practical application. In contrast to these methods, the use of cationic photoinitiator provides a convenient method of generating powerful acid catalysts in situ: the photoinduced organic-inorganic reactions can be triggered precisely and homogeneously by irradiation when desired and without processing or storage difficulties. Furthermore, UV technology obviates the difficulties of the sol-gel general process that starts in alcoholic solution including a catalyst and water. In our case, traces of water from air moisture turn out to be sufficient to initiate the hydrolysis reactions. Last, photoacids are true catalysts which are not incorporated into the polymer microstructure.

V. References

- 1 LÜling, M. *Injection Moulding* **1998**, 41
- 2 Schottner, G.; Rose, K.; Posset, U. *Journal of Sol-Gel Science and Technology* **2003**, 27, (1), 71-79.
- 3 Amberg-Schwab, S.; Hoffmann, M.; Bader, H.; Gessler, M. *Journal of Sol-Gel Science and Technology* **1998**, 13, (1/2/3), 141-146.
- 4 Amberg-Schwab, S.; Katschorek, H.; Weber, U.; Burger, A.; Haensel, R.; Steinbrecher, B.; Harzer, D. *Journal of Sol-Gel Science and Technology* **2003**, 26, (1/2/3), 699-703.
- 5 Schottner, G.; Kron, J.; Deichmann, A. *Journal of Sol-Gel Science and Technology* **1998**, 13, (1/2/3), 183-187.
- 6 Coudray, P.; Etienne, P.; Moreau, Y. *Materials Science in Semiconductor Processing* **2000**, 3, (5/6), 331-337.
- 7 Brusatin, G.; Della Giustina, G.; Guglielmi, M.; Innocenzi, P. *Progress in Solid State Chemistry* **2006**, 34, (2-4), 223-229.
- 8 Crivello, J. V.; Song, K. Y.; Ghoshal, R. *Chemistry of Materials* **2001**, 13, (5), 1932-1942.
- 9 Croutxé-Barghorn, C.; Soppera, O.; Carre, C. *Journal of Sol-Gel Science and Technology* **2007**, 41, (1), 93-97.
- 10 Sangermano, M.; Amerio, E.; Priola, A.; Di Gianni, A.; Voit, B. *Journal of Applied Polymer Science* **2006**, 102, (5), 4659-4664.
- 11 Soppera O., Croutxé-Barghorn C. *J. Polym. Sci. : Part A : Polym. Chem.*, **41**, 716-24 (2003).
- 12 O. Soppera O., Croutxé-Barghorn C. *J. Polym. Sci. : Part A : Polym. Chem.*, **41**, 831-40 (2003).
- 13 Highlink® Nano G Silica organosols from CLARIANT
- 14 Nanocryl® and Nanopox® from NANORESINS.
- 15 Bauer, F.; Flyunt, R.; Czihal, K.; Buchmeiser, M. R.; Langguth, H.; Mehnert, R. *Macromolecular Materials and Engineering* **2006**, 291, (5), 493-498.
- 16 Cho, J.-D.; Ju, H.-T.; Hong, J.-W. *Journal of Polymer Science, Part A: Polymer Chemistry* **2005**, 43, (3), 658-670.
- 17 Vu, C.; LaFerte, O.; Eranian, A. *European Coatings Journal* **2002**, (1-2), 64,66-68,70.
- 18 Xu, G. C.; Li, A. Y.; De Zhang, L.; Wu, G. S.; Yuan, X. Y.; Xie, T. *Journal of Applied Polymer Science* **2003**, 90, (3), 837-840.
- 19 Posthumus, W. UV-curable acrylate metal oxide nanocomposite coatings PhD dissertation. Technische Universiteit Eindhoven, Eindhoven, The Netherlands, 2004.
- 20 Decker C., Clay-acrylate nanocomposite photopolymers in *Polymer nanocomposites Y.W Mai, Z.Z Yu (ed), Woodhead Publishing*, Cambridge, 188-205 (2006).